# The Influence of Parameterized Ice Habit on the Glaciation of Arctic Clouds

JERRY Y. HARRINGTON[1]*, ALEXANDER AVRAMOV [2], DENNIS LAMB[1], KARA SULIA[1], AND CHENGZHU ZHANG[1]

[1] *Department of Meteorology, Pennsylvania State University, University Park, PA*

[2] *NASA Goddard Institute for Space Studies, New York, New York*

# 1 Introduction

Mixed-phase stratus clouds are prevalent in the Arctic during the winter and transition seasons (Curry et al., 1996; Intrieri et al., 2002). Due to the lower equilibrium vapor pressure of ice as compared to liquid, ice crystals in mixed-phase clouds grow at the expense of the cloud droplets (Wegener-Bergeron-Findeisen process, hereafter Bergeron process, Pruppacher and Klett, 1997, pgs. 548-549). Subsequent ice precipitation may then cause the complete glaciation and dissipation of the cloud. Nevertheless, the liquid phase is commonly found in Arctic clouds (Pinto, 1998; Hobbs and Rangno, 1998; Prenni et al., 2007) to temperatures as low as -31 °C (Hobbs and Rangno, 1998, e.g.). These cloud systems can persist from a few days to a couple of weeks. Capturing this persistence poses modeling challenges and is important in part because the radiatively-important liquid phase affects the surface energy budget (Shupe and Intrieri, 2004; Prenni et al., 2007) and, consequently, the freezing and melting rate of the Arctic sea ice (Jiang et al., 2000; Francis et al., 2005; Kay and Wood, 2008).

At present, how mixed-phase Arctic clouds can maintain supercooled liquid for extended periods of time is not completely understood, though several hypotheses have been advanced. Small crystal sizes at cloud top (Rauber and Tokay, 1991), strong dynamic forcing (Korolev and Isaac, 2003; Korolev, 2007), and low ambient ice nuclei (IN) concentrations (Pinto, 1998; Harrington et al., 1999; Jiang et al., 2000, e.g.,) have all been advanced as reasons for mixed-phase cloud persistence though it seems likely that all of these mechanisms work in tandem. For instance, Harrington et al. (1999) hypothesized that mixed-phase clouds are maintained through a balance between liquid water production resulting from cloud-top radiative cooling and turbulent fluxes of vapor from below in conjunction with ice sedimentation. In addition, Harrington et al. (1999) suggested that this balance depends on the low average ambient deposition/condensation IN concentrations in the Arctic ($< 1\,\mathrm{l}^{-1}$, Bigg, 1996; Rogers et al., 2001) and on IN removal by sedimentation Harrington and Olsson (2001).

The rapid removal of deposition/condensation-freezing IN tends to produce clouds with ice water contents (IWCs) and ice concentrations that are too low in comparison to observations (e.g. Morrison et al., 2005; Fridlind et al., 2007; Morrison et al., 2008). A number of hypothesis have been advanced to explain the discrepancies. Similarly to Carrio et al. (2005), Avramov and Harrington (2006) suggest that IN-rich air from above the boundary layer is entrained leading to continual ice production. Morrison et al. (2005) suggest that the persistence of, and continual production of ice in, Arctic mixed-phase clouds involves a self-regulating negative feedback due to drop freezing by contact nucleation. In contradistinction, Avramov and Harrington (2006) could not produce significant IWCs by contact nucleation unless the contact IN concentrations were as high as those reported by Young (1974), which are considered to be too large (e.g. Meyers et al., 1992). In order to maintain liquid while obtaining realistic ice concentrations, Fridlind et al. (2007) parameterized two relatively controversial nucleation mechanisms. The first mechanism, "evaporation nucleation," hypothesizes that a fraction of all evaporating supercooled drops freeze (Cotton and Field, 2002). The second hypothesis, "evaporation IN," suggests that IN are released during drop evaporation (Rosinski and Morgan, 1991). Fridlind et al. (2007) shows that only these two mechanisms can produce liquid and ice amounts that consistently match observations.

While most prior studies focus primarily on ice nucleation and ice concentrations, it is also feasible that how ice habit is parameterized could influence the simulated structure of mixed-phase clouds. The Bergeron process depends not only on the ice concentration but also on the in-cloud residence time and vapor growth rate, both of which depend on habit and size (Chen and Lamb, 1994; Fukuta and Takahashi, 1999, e.g.,). Indeed, in a simplified example Harrington et al. (1999) showed that different habits can have an impact on simulated mixed-phase clouds. Moreover, many models use different parameterizations for ice habit which may lead to differences in the model results. In this paper, we examine the influence that parameterized ice habit has on the evolution of mixed-phase Arctic stratus. We also discuss the implications, and limitations, of current crystal growth models for our results.

# 2 Case and Model Description

We focus on two periods from the Mixed-Phase Arctic Cloud Experiment (M-PACE, Verlinde et al., 2007) - the period from 12Z on October 5 to 12Z on October 8 (case A), and the period from 17Z on October 9 to 5Z on October 10, 2004 (case B). Case B was a single layer mixed-phase cloud (Klein et al.,

*Corresponding author address: J.Y. Harrington, Department of Meteorology, Pennsylvania State University, 503 Walker Building, University Park, PA 16802; *e-mail*: harring@mail.meteo.psu.edu.

2009) whereas case A had multiple liquid layers with ice crystals falling between them (Morrison et al., 2009). Surface-based measurements were taken for both cases at Barrow, Alaska and at Oliktok point ( 220 km east of Barrow) and in-situ aircraft measurements were also taken (McFarquhar et al., 2007).

The model used in this study is the Colorado State University version of the Regional Atmospheric Modeling System (Cotton et al., 2003, RAMS CSU) with two-moment bulk microphysics (Meyers et al., 1997). The RAMS model was configured as a 2-D cloud-resolving model for the recent M-PACE intercomparison studies (Klein et al., 2009; Morrison et al., 2009). The computational domain has 150 horizontal grid points with 1 km spacing and 72 vertical grid points with 25 m spacing in the boundary layer, stretching to 1000 m at the domain top. The model is initialized with a prescribed sounding along with imposed large-scale forcing and surface fluxes developed specifically for the M-PACE intercomparison. The lower boundary is assumed to be snow-covered land (case A, multi-layer) or ocean (case B, single layer). The simulation duration of case A is 72 hours and case B is 12 hours, with a 2 second time-step.

The microphysical model has seven hydrometeor categories: cloud droplets, rain, pristine ice, snow, aggregates, graupel and hail. Both mixing ratio and number concentration are predicted for all categories, except cloud droplets for which the number concentration is prescribed. Pristine ice and snow categories are primarily vapor grown and together allow for a bi-modal ice crystal size distribution. The pristine ice category represents small crystals (mean maximum dimension $<$ 125 $\mu$ m) into which ice nucleates. Snow is defined as larger ice crystals ($>$ 125 $\mu$ m) which grow by vapor deposition and a small amount of riming. Ice is converted between snow and pristine ice by vapor diffusion. Aggregates form by collection between pristine ice, snow, and aggregates. Graupel is assumed to be spherical and is formed by riming or partial melting of pristine ice, snow and aggregates.

Pristine ice crystals are formed by homogeneous and heterogeneous nucleation. The model explicitly includes condensation/deposition-freezing and contact freezing nucleation, whereas immersion freezing is assumed to be implicit in the deposition/condensation-freezing (hereafter deposition freezing) parameterization of Meyers et al. (1992) and possibly in the IN measurements from M-PACE (Prenni et al., 2007, and Paul DeMott, personal communication). The number of IN acting in the deposition freezing mode is parameterized as a function of ice supersaturation following Meyers et al. (1992),

$$N_i = exp(a + bs_i), \qquad (1)$$

where Ni is the number of nucleated crystals ($\mathrm{l}^{-1}$), $s_i$ is the ice supersaturation (%) and $a$ and $b$ are empirically-derived coefficients. The coefficients in Eq. 1 were modified using M-PACE IN data (Prenni et al., 2007, see) with coefficient values of $a$ and $b$ ($a$ = -1.488, $b$ = 0.0187). The modified parameterization predicts IN concentrations of nearly 0.15 $\mathrm{l}^{-1}$ at water saturation for our cases (see sections below), which is consistent with other Arctic IN measurements (Bigg, 1996; Rogers et al., 2001, e.g.) and a factor of 26 lower than the standard Meyers parameterization. Contact nucleation is computed following Meyers et al. (1992) except that the contact IN concentration is arbitrarily reduced by a factor of 26 for consistency with the reduction in deposition IN. The concentrations of IN are prognosed in our simulations through a method of nucleation-scavenging following Avramov and Harrington (2006); Prenni et al. (2007).

The parameterized ice habit is important for simulated mixed-phase cloud evolution because liquid depletion by the ice crystals depends on the vapor growth rate and the fall-speed, both of which depend on habit. The fall-speed of the crystals is parameterized following Mitchell (1996),

$$v_t = \alpha_v D^{\beta_v}, \qquad (2)$$

where D is the crystal maximum dimension and $\alpha_v$ and $\beta_v$ are empirically-derived coefficients, which differ for each crystal habit. The vapor growth rate for a single crystal is (c.f., Walko et al., 1995; Pruppacher and Klett, 1997, pg. 547),

$$\frac{dm}{dt} = 2\pi D S(\phi) D_v f_{Re}(v_t)(\rho_{v,\infty} - \rho_{v,i}), \qquad (3)$$

where $D_v$ is the vapor diffusivity, $m$ is crystal mass, $\rho_{v,\infty}$ is the ambient vapor density, $\rho_{v,i}$ is the ice equilibrium vapor density, $S(\phi)$ is the shape factor which is defined as $S = C/D$ with C the crystal capacitance, and $f_{Re}(v_t)$ is the ventilation coefficient which depends on the fall-speed. The shape factor, $S$, is fixed during a simulation even though it changes with crystal aspect ratio (Chen and Lamb, 1994, $\phi$, e.g.). Prognosis of the crystal mass requires a functional relationship between mass and size. Many models use a mass relationship like that given by Mitchell (1996),

$$m = \alpha_m D^{\beta_m} \qquad (4)$$

where $\alpha_m$ and $\beta_m$ are empirically-derived coefficients for each habit. As a consequence of the mass relationship and crystal capacitance, different crystal shapes have different growth characteristics. In general, more extreme aspect ratios lead to a larger capacitance, and faster vapor growth (e.g., Chen and Lamb, 1994). For instance, dendrites grow faster than hexagonal plates because of the greater capacitance, extreme aspect ratio, and larger size of the dendrites(e.g. Chen and Lamb, 1994; Fukuta and Takahashi, 1999; Sheridan, 2008; Sheridan et al., 2009).

# 3 Mass and Fall-Speed Relations

To investigate the influence of parameterized habit on mixed-phase cloud simulations we performed a series of sensitivity studies using different crystal shapes. This study was motivated in part by prior simulations which produced faster glaciation (Harrington et al., 1999; Prenni et al., 2007) as compared to other studies using similar IN concentrations (e.g., Fridlind et al., 2007; Morrison et al., 2008). Three crystal shapes were used in the simulation: hexagonal plates, dendrites and spheres. Dendrites and hexagonal plates were chosen because many models assume plate-like crystals in the temperature and supersaturation ranges for the clouds we simulated (-11 to -16 $^\circ$C). Spherical shapes were included in part because they are the most compact "crystal" for a given size and have the largest fall-speed. Consequently, spheres provide the greatest contrast to dendrites, which have the largest growth rate, but smallest fall-speed for a given size. In addition, including spheres in our simulations allows us to compare our results to studies that used a spherical shape (Fridlind et al., 2007; Morrison et al., 2008). Our habit choices, as we discuss below, cover the range from the fastest growing crystals, but slowest falling (dendrites) to the slowest growing crystals, but fastest falling (spheres)

The mass and fall-speed relationships reported in the literature for ice span a relatively large range (Pruppacher and Klett, 1997; Mitchell, 1996; Heymsfield and Kajikawa, 44; Heymsfield et al., 2002). Hence, we examine the sensitivity of model-simulated mixed-phase clouds to the span in these relations which are shown as the grey areas on Figs. 1. For spheres, the span is produced by using similar relationships to those of Fridlind et al. (2007) and Morrison et al. (2008) (formula from personal communication). For our simulations, we select relations that define the maximum and minimum, or the extremes, for each mass and fall-speed range. The sensitivity of the simulated cloud with respect to crystal habit is then investigated using these extremes. Physically, the extremes of each range refer to the density, or the compactness, of the crystal: The curves that define the upper range of the mass and fall-speed relations are associated with high-density crystals in the case of spheres and dendrites (broad-branched stellars), and thick plates in the case of hexagonal crystals. Similarly, the curves defining the lower range are associated with low-density crystals, in the case of spheres and dendrites (classic dendrites), and thin plates in the case of hexagonal crystals. These terms for the extremes will be used throughout the paper.

How compact, or dense, a crystal is has important consequences for vapor growth. For the same volume, more compact, dense crystals have weaker vapor growth rates (e.g., Chen and Lamb, 1994; Fukuta and Takahashi, 1999; Sheridan et al., 2009). To illustrate this dependence, the growth of an equivalent volume sphere is compared to predictions from the adaptive habit model of Chen and Lamb (1994). The Chen and Lamb (1994) model was used because it accurately simulates the evolution of crystal mass and aspect ratio at water saturation. After 20 min of growth, the mass of an equivalent volume sphere is significantly smaller than the accurate model except at the transition temperatures between habits (-9 and -22 °C) where habit growth is roughly isometric (Fig. 2). Consequently, we should expect more isometric, and compact, crys-

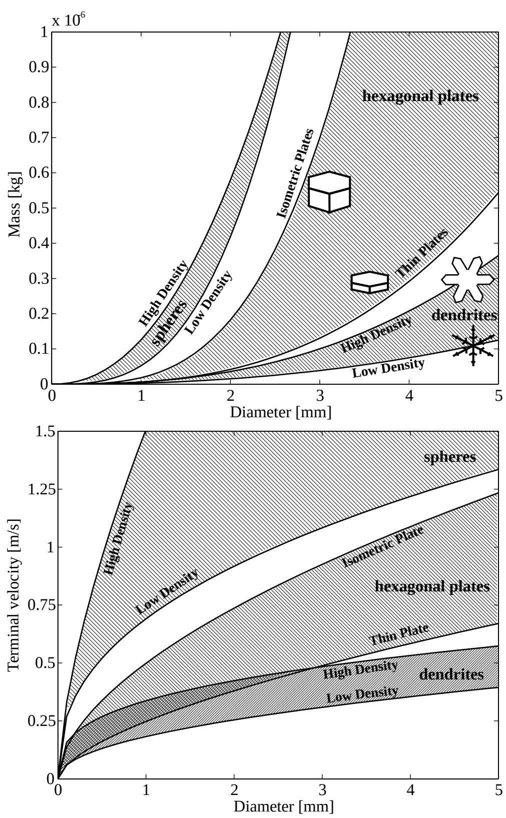


Figure 1: Ranges of (a) mass-dimensional and (b) fall-speed relations of the crystal habits used in the simulations. The extremes of the range for each habit are defined by the highest and lowest density particles for spheres and dendrites, and by the thickest and thinnest plates for hexagonal plates. The terms “high density” or “thick plate” and “low density” or “thin plate” are used to refer to the extremes for each range

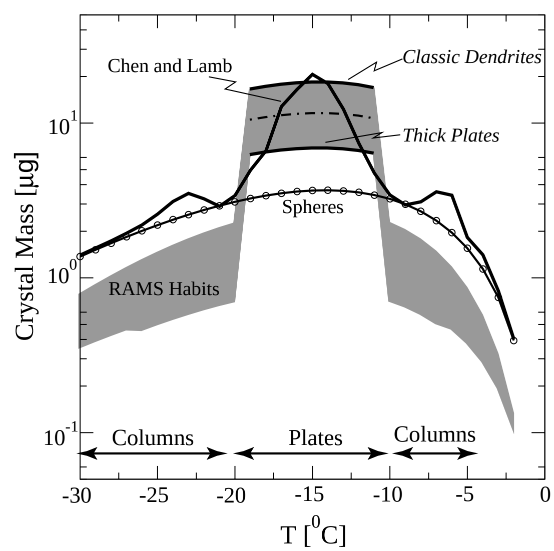


Figure 2: Crystal mass as a function of temperature for a single particle grown for 20 min at water saturation. The solid line is from the Chen and Lamb (1994) spheroid approximation to crystal growth, which is considered to be relatively accurate at water saturation. The solid-circle line is for equivalent volume spheres using the reduced density from Chen and Lamb (1994) (their Eq. 42). The gray areas indicate the range of masses predicted using the RAMS mass and capacitance. In the plate regime, RAMS low-density (classic) dendrites define the upper edge of the grey area whereas the lower edge is defined by thick plates. The dash-dotted line is for thin plates and high-density (stellar) dendrites, which have very similar model growth rates.

tals to grow more slowly in time leading to a weaker Bergeron process.

# 4 Simulation Results: Comparison with Observations

Our baseline simulations for the single and multi-layer cases examine the combinations of physical factors (IN concentration and habit) necessary to produce the best overall comparison with data taken during M-PACE. We undertake these studies precisely because of the large range of mass and fall-speed relations available (Fig. 1). Furthermore, the baseline results provide a framework for discussions of the sensitivities to habit parameterization. The observed liquid water path (LWP) data are derived from microwave radiometer measurements (Turner et al., 2007) and are averaged for the three sites Atqasuk, Barrow and Oliktok. The best match between the simulations and the observed LWP was obtained with high-density dendrites (stellars) and M-PACE IN concentrations (Fig. 3). The simulation with high-density dendrites produces LWP oscillations that follow the observations remarkably well and range between 90 and 170 g m$^{-2}$. An analysis of the simulation (not shown) suggests that the oscillations in the LWP are caused by the entrainment of IN-rich air from above the cloud, producing ice precipitation and a decrease of the LWP similar to Carrio et al. (2005). The IN depletion by ice sedimentation allows for a consequent LWP increase similar to Harrington and Olsson (2001).

Similar to the single layer case, the simulations for each habit were compared with the ground-based LWP retrievals ofTurner et al. (2007) and airborne measurements (data from DOE-ARM archive) as shown on Fig. 4. No clouds were produced by any simulation for the first 10 hours. The simulation with high-density dendrites used M-PACE IN concentrations and over-estimated the peaks in the LWP during the first and final 24 hours, and under-estimated the LWP in the middle of

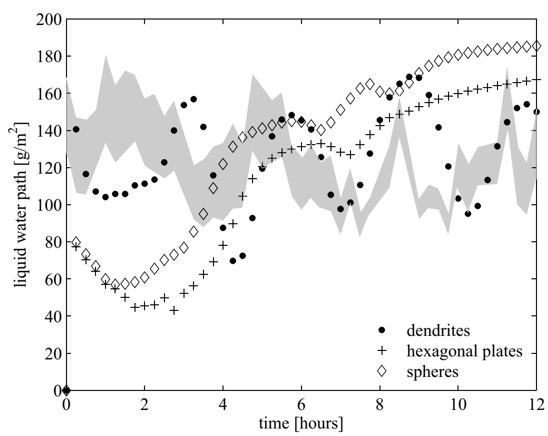


Figure 3: Time series of simulated (symbols) and retrieved (shaded) liquid water path [g m$^{-2}$] for the single layer case. Simulated quantities are domain averaged. Shaded area represents the 95% confidence interval of observational data.

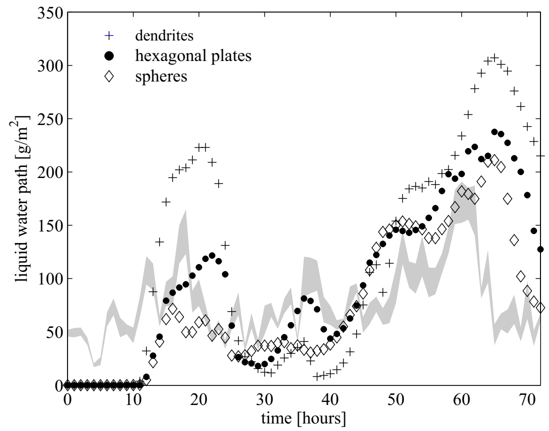


Figure 4: Time series of simulated (symbols) and retrieved (shaded) liquid water path [g m$^{-2}$] for the multi-layer case. Simulated quantities are domain averaged. The shaded area represents the 95% confidence interval of observational data.

the simulation. As in the single-layer case, IN concentrations were increased by 25 times the M-PACE values so that spheres and thick plates could be brought into better agreement with the observations. The best correspondence with observations was achieved using thick plates in which the simulated LWP followed the observations reasonably well.

# 5 Sensitivity to Mass and Fall Speed Relations

To illustrate the overall influence of mass and fall-speed choice on simulated phase-partitioning, we computed simulation-averaged LWP and IWP for all IN concentrations and for each sensitivity simulation. The range of possible LWP and IWP produced by using the four combinations of mass and fall-speed relations for each habit are shown on Fig. 5 for the single-layer case. We do not show the sensitivities for the multi-layered case as they are similar.

Simulations with hexagonal plates and spheres produced similar results (Fig. 5) though with a different spread: The LWP was greatest and the IWP smallest for these habits. At low IN concentrations both hexagonal plates and spheres do not show much sensitivity to the mass and fall-speed relations. As the IN concentration increases, the range of LWP and IWP variation also increases, reaching relative differences of up to 60% and 75%, respectively. The respective upper and lower bounds of the LWP range are defined by simulations with high-density or thick (slow vapor growth, fast falling) and low-density or thin (fast vapor growth, slow falling) crystals. Simulations using thick plates or high-density spheres produced the largest LWP and smallest IWP whereas the converse is true for low-density spheres and thin plates. Physically, this makes sense because more compact, isometric particles have lower vapor growth rates at our cloud temperature ( -15 °C, see Fig. 2) but greater fall-speeds (e.g., Fukuta and Takahashi, 1999). As

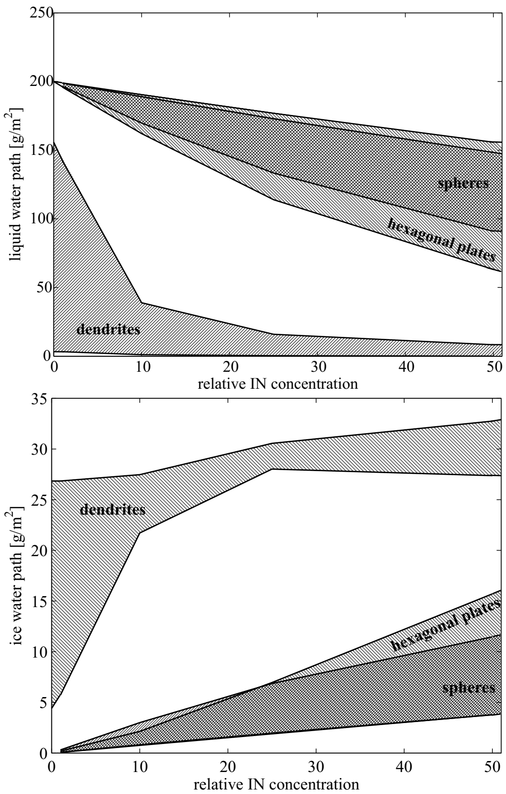


Figure 5: Ranges of simulated (a) liquid and (b) ice water path [g m$^{-2}$] for different habits as a function of IN concentration for the single layer case. Simulated quantities are domain and simulation averaged. IN concentration is relative to 0.15 l$^{-1}$.

Fig. 2 shows, both thick and thin plates in RAMS have produce growth rates that are lower than those computed with an accurate ice crystal growth model. Spheres tend to define the upper limit in Fig. 5a: They are the fastest- falling particles with the slowest vapor growth rates (Fig. 2) and consequently more liquid can be maintained. The large difference in vapor growth rates and fall-speeds for each habit is also the reason for the different IN sensitivity for each habit: The change in LWP with a relative IN increase from one to 50 for thin plates is 68%, as compared to only 22% in the case of the thick plates. These results are similar to the low IN-sensitivities reported by studies that use high density, fast-falling, and slowly growing ice habits (Fridlind et al., 2007; Morrison et al., 2008).

In contrast to simulations with hexagonal plates and spheres, simulations with dendrites show a stronger IN sensitivity. At low IN concentrations ($< 1$ l$^{-1}$) simulations with high-density dendrites produced a LWP and IWP which is closer to the simulations with spheres and hexagonal plates (upper curve on the dendrite range in Fig. 5a). Increasing the IN concentration leads to a larger reduction in the LWP as compared to spheres or hexagonal plates, and is similar to prior studies with dendrites (Harrington and Olsson, 2001; Jiang et al., 2000; Prenni et al., 2007). In the case of low-density (classic) dendrites, the LWP is negligible even at low IN concentrations (lower curve on the dendrite range in Fig. 5a). The large range of sensitivity for dendrites makes physical sense. Dendrites have the largest vapor growth rates, but the lowest fall-speed, of any habit. This is clearly indicated on Fig. 2 by the Chen and Lamb (1994) result at -15 °C. In addition, the mass relation used in RAMS for dendrites and plates leads to a significant range of possible crystal growth rates (shaded region, Fig. 2). Thus, it should be expected that a large sensitivity to changes in the mass relationship, and a wide range of possible LWP and IWP (Fig. 5), would exist. The water path ranges are greatest at low IN concentrations for dendrites because crystal sizes are the largest here, leading to the strongest vapor growth, the largest liquid depletion rates, and hence the largest sensitivity to the mass relations.

# 6 Missing Model Physics: Habits and Surface Kinetics

Though the uncertainty in the mass-dimensional relationships has a strong influence on mixed-phase cloud glaciation there are other physical processes that are lacking in cloud models. For instance, non-spherical ice crystal growth models like those used in RAMS (Walko et al., 1995) produce crystal masses within the shaded range shown on Fig. 2. The reason for this range is due primarily to the fact that ice crystals in RAMS use a single mass-dimensional relationship for a given primary habit. As a consequence, ice growth matches the Chen and Lamb (1994) adaptive habit model well near -15 °C but overestimates growth for most other temperatures within the platelike growth regime ($T$ = -9 to -22 °C). This indicates that a cloud model like RAMS will over-estimate the rates of glaciations of clouds as the transition temperatures between habits (-9 and -22 °C) are approached.

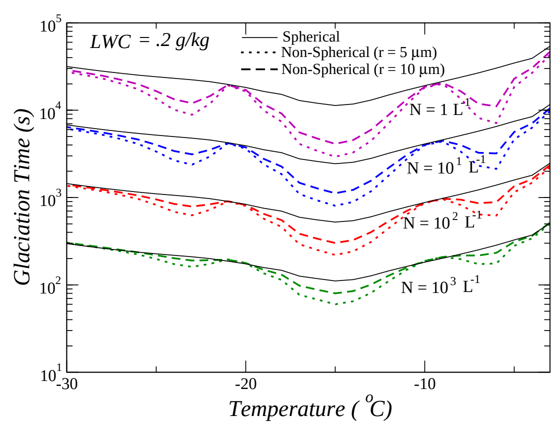


Figure 6: Glaciation time-scales computed with the Chen and Lamb (1994) model at water saturation, 850 hPa pressure, and constant temperature. An initial gamma distribution of ice crystals (initial mean size indicated on the figure) is grown until the IWC reaches 0.2 g/kg. The time-scale for this process is equivalent to the glaciation time-scale for ice crystals growing at the expense of liquid drops in a static environment.

To complicate matters further, the time required to glaciate a cloud (glaciation time-scale, $\tau_g$) appears to depend on the initial size of the ice crystals. For instance, Fig. 6 shows values of $\tau_g$ estimated from a box-model calculation. The box model grows ice crystals at water saturation, with temperature and pressure held constant, until a specified water content is reached. The procedure is similar to that of Korolev and Isaac (2003) except that the adaptive habit ice crystal growth model of Chen and Lamb (1994) was used. The figure shows that the glaciation time depends not only on ice concentration but also on ice habit (dashed curve), and that glaciation is much more rapid where plate and column growth is the greatest. Moreover, the figure also shows a distinct influence on the initial size of the ice crystals. The dotted line shows results for model calculations that assumed an initial ice distribution of particles with a mean size of 10 $\mu$m whereas the dashed line shows results with an initial means size of 5 $\mu$m. While the habit influence as compared to spherical ice growth certainly dominates, the influence of the initial size of the ice also appears to be important. As Sheridan et al. (2009) show, this result is due to the fact that smaller crystals have a larger relative increase in mass during growth, which results in a larger increase in crystal aspect ratio. The greater aspect ratio, in turn, produces larger vapor gradients and stronger crystal growth.

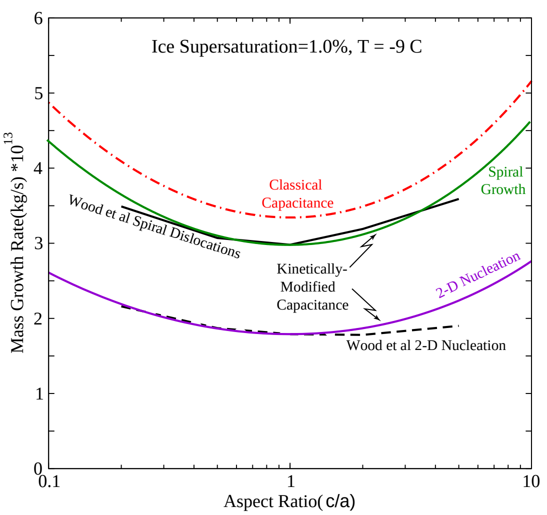


Figure 7: Growth rate as a function of aspect ratio at low ice supersaturations computed with the standard capacitance model, new kinetically-modified capacitance model, and model output from the hexagonal plate model of Wood and Baker (2001). Kinetically-modified growth assumed either spiral dislocations or 2-D nucleation when the particle deposition coefficient was computed. A critical supersaturation of 0.565% was assumed for each growth mechanism

While the capacitance model is used routinely in cloud modeling, it has long been known that the model over-estimates vapor growth at low ice supersaturations (e.g. Nelson and Baker, 1996; Wood and Baker, 2001). It has been suggested that the over-estimates in vapor growth are due to two factors. First of all, the capacitance model has the wrong boundary condition for faceted growth (constant density instead of constant flux), and, second, the capacitance model does not include the influences of surface kinetic resistance due to deposition coefficients that are less than unity. However, it is possible to modify the capacitance model so that surface kinetic resistance is taken into account. We have recently re-derived the capacitance model including surface kinetic resistance following the approach outlined in Lamb and Chen (1995). The surface kinetic resistance model requires knowledge of whether growth occurs through permanent spiral dislocations or two-dimensional (2-D) nucleation of ledges on the crystal surface. We have included both processes and compare our results with those from a detailed model of hexagonal growth (Wood and Baker, 2001). Note that the standard capacitance growth model over-estimates growth at an ice supersaturation of 1%. However, including surface kinetic resistance in the capacitance model causes a reduction in the ice crystal growth rates. Particularly impressive is the fact that the kinetically-limited capacitance model compares favorably to the Wood and Baker (2001) model for both spiral growth and 2-D nucleation.

# 7 Concluding Remarks

The results from this sections indicate that the ice crystal vapor growth equations, as currently parameterized in cloud models, have serious deficiencies. The range of mass-dimensional relations used in cloud models to parameterize ice growth produces a large range of possible liquid and ice water paths for simulated mixed-phase clouds. Moreover, ice habit growth depends on temperature and this is not captured well by either spherical growth, or by the ice crystal growth models used in RAMS. Furthermore, ice crystal growth and mixed-phase cloud glaciation appear to depend on the initial size of the ice. Finally, the capacitance model over-estimates ice crystal growth at low ice supersaturations because of the lack of surface kinetic-resistance. In order to improve ice crystal growth in cloud models all of these physical processes need to be taken into account.

*Acknowledgments.* The authors would like to thank the National Science Foundation for support under grant No. ATM-0639524, and the Office of Biological and Environmental Research of the U.S. Department of Energy (DE-FG02-05ER64058) as part of the Atmospheric Radiation Measurement Program

# References

Avramov, A. and J. Harrington, 2006: The influence of ice nucleation mode and ice vapor growth on simulation of arctic mixed-phase clouds. *12$^{th}$ Conference on Cloud Physics*, Madison, WI, American Meteorological Society.

Bigg, E., 1996: Ice forming nuclei in the high arctic. *Tellus*, **48**, 223–233.

Carrio, G., H. Jiang, and W. Cotton, 2005: Impact of aerosol intrusions on arctic boundary layer clouds. Part I: 4 May 1998 case. *J. Atmos. Sci.*, **62**, 3082–3093.

Chen, J. and D. Lamb, 1994: The theoretical basis for the parameterization of ice crystal habits: Growth by vapor deposition. *J. Atmos. Sci.*, **51**, 1206–1221.

Cotton, R. J. and P. R. Field, 2002: Ice nucleation characteristics of an isolated wave cloud. *Quart. J. Roy. Meteor. Soc.*, **128**, 2417–2437.

Cotton, W., R. Pielke, R. Walko, G. Liston, C. Tremback, J. Harrington, and H. Jiang, 2003: Rams 2000: Current status and future directions. *MAP*, **82**, 5–29.

Curry, J. A., W. B. Rossow, D. Randall, and J. L. Schramm, 1996: Overview of arctic cloud and radiation characteristics. *J. Climate*, **9**, 1731–1764.

Francis, J. A., E. Hunter, J. R. Keu, and X. Wang, 2005: Clues to variability in arctic minimum sea ice extent. *Geophys. Res. Let.*, **32**, L21 501, doi:10.1029/2005GL024376.

Fridlind, A., A. Ackerman, G. McFarquhar, G. Zhang, M. Poellot, P. DeMott, A. Prenni, and A. Heymsfield, 2007: Ice properties of single-layer stratocumulus during the Mixed-Phase Arctic Cloud Experiment (M-PACE): Part II, Model results. *J. Geophys. Res.*, **112**, D24 202, doi:10.1029/2007JD008646.

Fukuta, N. and T. Takahashi, 1999: The growth of atmospheric ice crystals: A summary of findings in vertical supercooled cloud tunnel studies. *J. Atmos. Sci.*, **56**, 1963–1979.

Harrington, J. Y. and P. Q. Olsson, 2001: On the potential influence of ice nuclei on surface-forced marine stratocumulus cloud dynamics. *J. Geophys. Res.*, **106**, 27,473–27,484.

Harrington, J. Y., T. Reisin, W. R. Cotton, and S. M. Kreidenweis, 1999: Cloud resolving simulations of Arctic stratus. Part II: Transition-season clouds. *Atmos. Res.*, **51**, 45–75.

Heymsfield, A. J., A. Bansemer, S. Lewis, J. Iaquinta, M. Kajikawa, C. Twohy, M. R. Poellot, and L. M. Miloshevich, 2002: A general approach for deriving the properties of cirrus and stratiform ice cloud particles. *J. Atmos. Sci.*, **59**, 3–29.

Heymsfield, A. J. and M. Kajikawa, 44: An improved approach to calculating terminal velocities of plate-like crystals and graupel. *J. Atmos. Sci.*, 1088–1099.

Hobbs, P. V. and A. L. Rangno, 1998: Microstructure of low and middle-level clouds over the beaufort sea. *Quart. J. Roy. Meteor. Soc.*, **124**, 2035–2071.

Intrieri, J. M., M. D. Shupe, T. Uttal, and B. J. McCarty, 2002: An annual cycle of arctic cloud characteristics observed by radar and lidar at SHEBA. *J. Geophys. Res.*, **107**, doi:10.1029/2000JC000423.

Jiang, H., W. R. Cotton, J. O. Pinto, J. A. Curry, and M. J. Weissbluth, 2000: Sensitivity of mixed-phase arctic stratocumulus to ice forming nuclei and large-scale heat and moisture advection. *J. Atmos. Sci.*, **57**, 2105–2117.

Kay, J. and R. Wood, 2008: Timescale analysis of aerosol sensitivity during homogeneous freezing and implications for upper tropospheric water vapor budgets. *Geophys. Res. Let.*, **35**, doi: 10.1029/2007GL032628.

Klein, S., et al., 2009: Intercomparison of model simulations of mixed-phase clouds observed during the ARM Mixed-Phase Arctic Cloud Experiment. Part I: Single layer cloud. *Quart. J. Roy. Meteor. Soc.*, accepted.

Korolev, A., 2007: Limitations of the wegener-bergeron-findeisen mechanism in the evolution of mixed-phase clouds. *J. Atmos. Sci.*, **64**, 3372–3375.

Korolev, A. V. and G. A. Isaac, 2003: Phase transformation in mixed-phase clouds. *Quart. J. Roy. Meteor. Soc.*, **129**, 19–38.

Lamb, D. and J. Chen, 1995: An expanded parameterization of growth of ice crystals by vapor deposition. *Conference on Cloud Physics*, Dallas, Texas, AMS, Boston, 15-20 January, 389-392.

McFarquhar, G. M., G. Zhang, M. R. Poellot, G. L. Kok, R. McCoy, T. Tooman, A. Fridlind, and A. J. Heymsfield, 2007: Ice properties of single-layer stratocumulus during the Mixed-Phase Arctic Cloud Experiment. 1. Observations. *J. Geophys. Res.*, **112**, D24 201, doi: 10.1029/2007JD008633.

Meyers, M. P., P. J. DeMott, and W. R. Cotton, 1992: New primary ice-nucleation parameterizations in an explicit cloud model. *J. Appl. Meteor.*, **31**, 708–721.

Meyers, M. P., R. L. Walko, J. Y. Harrington, and W. R. Cotton, 1997: New rams cloud microphysics parameterization. Part II: The two-moment scheme. *Atmos. Res.*, **45**, 3–39.

Mitchell, D. L., 1996: Use of mass- and area-dimensional power laws for determining precipitation particle terminal velocities. *J. Atmos. Sci.*, **53**, 1710–1723.

Morrison, H., J. O. Pinto, J. A. Curry, and G. M. McFarquhar, 2008: Sensitivity of modeled arctic mixed-phase stratocumulus to cloud condensation and ice nuclei over regionally varying surface conditions. *J. Geophys. Res.*, **113**, D05 203, doi:10.1029/2007JD008729.

Morrison, H., M. Shupe, J. Pinto, and J. Curry, 2005: Possible roles of ice nucleation mode and ice nuclei depletion in the extended lifetime of arctic mixed-phase clouds. *Geophys. Res. Let.*, **32**, doi: 10.1029/2005GL023614.

Morrison, H., et al., 2009: Intercomparison of model simulations of mixed-phase clouds observed during the arm mixed-phase arctic cloud experiment, Part II: Multi-layered cloud. *Quart. J. Roy. Meteor. Soc.*, accepted.

Nelson, J. and M. Baker, 1996: New theoretical framework for studies of vapor growth and sublimation of small ice crystals in the atmosphere. *J. Geophys. Res.*, **101**, 7033–7047.

Pinto, J. O., 1998: Autumnal mixed-phase cloudy boundary layers in the arctic. *J. Atmos. Sci.*, **55**, 2016–2038.

Prenni, A., et al., 2007: Can ice-nucleating aerosols affect arctic seasonal climate? *Bull. Amer. Meteor. Soc.*, **88**, 541–550.

Pruppacher, H. R. and J. D. Klett, 1997: *Microphysics of Clouds and Precipitation*. Kluwer Academic Publishers, Boston, 954 pp.

Rauber, R. and A. Tokay, 1991: An explanation for the existence of supercooled water at the top of cold clouds. *J. Atmos. Sci.*, **48**, 1005–1023.

Rogers, D., P. DeMott, and S. Kreidenweis, 2001: Airborne measurements of tropospheric ice-nucleating aerosol particles in the arctic spring. *J. Geophys. Res.*, **106**, 15 053–15 063.

Rosinski, J. and G. Morgan, 1991: Cloud condensation nuclei as a source of ice-forming nuclei in clouds. *J. Aerosol. Sci*, **22**, 123–133.

Sheridan, L., 2008: Deposition coefficient, habit, and ventilation influences on cirriform cloud properties. M.S. thesis, The Pennsylvania State University, University Park PA, 16801, USA.

Sheridan, L., J. Harrington, D. Lamb, and K. Sulia, 2009: Habit influences on ice size spectra evolution during vapor diffusional growth. *J. Atmos. Sci.*, submitted.

Shupe, M. and J. Intrieri, 2004: Cloud radiative forcing of the arctic surface: The influence of cloud properties, surface albedo, and solar zenith angle. *J. Climate*, **17**, 616–628.

Turner, D., S. Clough, J. Liljegren, E. Clothiaux, K. Cady-Pereira, and K. Gaustad, 2007: Retrieving liquid water path and precipitable water vapor from Atmospheric Radiation Measurement (ARM) microwave radiometers. *IEEE Trans. Geosci. Remote Sens.*, **45**, 3680–3690.

Verlinde, J., et al., 2007: The mixed-phase arctic cloud experiment (M-PACE). *Bull. Amer. Meteor. Soc.*, **88**, 205–221.

Walko, R. L., W. R. Cotton, M. P. Meyers, and J. Y. Harrington, 1995: New RAMS cloud microphysics parameterization. Part I: The single moment scheme. *Atmos. Res.*, **38**, 29–62.

Wood, S. and M. Baker, 2001: New model for the vapor growth of hexagonal ice crystals in the atmosphere. *J. Geophys. Res.*, **106**, 4845–4870.

Young, K., 1974: The role of contact nucleation in ice phase initiation in clouds. *J. Atmos. Sci.*, **31**, 768–776.